

# Columbia University REU at Fermilab 2005

L. Gladstone

Summer 2005

The MiniBooNE experiment [1] is a  $\nu_\mu \rightarrow \nu_e$  oscillation search at Fermi National Accelerator Laboratory designed to confirm or rule out the LSND signal [2]. The Fermilab Booster accelerates protons to 8 GeV; these protons strike a beryllium target, generating mesons which decay to produce the MiniBooNE  $\nu_\mu$  beam. The neutrinos interact in a 12 m diameter sphere filled with mineral oil of food-grade purity, and the Čerenkov light from charged particles produced in these interactions is detected by 8 inch Hamamatsu [3] photomultiplier tubes (PMTs) lining the sphere. There are 1280 PMTs in the light-tight inner signal region: 956 are Hamamatsu model R1408, inherited from the LSND experiment; the remainder are Hamamatsu model R5912. Light produced in the outer concentric veto region is detected by an additional 240 R5912 PMTs. A typical tube is pictured in Figure 1. Light signatures recorded by the PMTs are used to reconstruct events within the detector. Leptons from charged current neutrino interactions are of particular interest, since these leptons tag the incoming neutrino flavor.

It is important to sufficiently understand the operating characteristics of the PMTs, since they are the only active detector element in MiniBooNE. MiniBooNE uses a Monte Carlo simulation to understand the detector's response to neutrino interactions. This program simulates photons traveling through the detector from creation to detection, and models all intermediate processes. The geometry of all detector elements is coded into the simulation, including that of the PMTs.

Photons striking the photocathode in a PMT produce photoelectrons (PEs), whose number is amplified via a dynode chain; the magnitude of the current so produced is proportional to the number of incident photons whose energy is above a certain threshold. A specific operating voltage had been found for each PMT so that all tubes have the proper gain. Gain is defined here as observed output charge (divided by charge per electron) per input photoelectron. The charge and timing information recorded from each PMT can then be used to reconstruct the events off-line. Ideally, this information,

along with photocathode efficiency as determined by Hamamatsu, specifies exactly when and how many photons hit the PMT. Each PMT had been tested in several ways to determine: basic functionality, timing resolution, charge resolution, dark rate and operating voltage. The operating voltage was chosen so that the gain is closest to the desired  $1.6 \times 10^7$  signal electrons per photoelectron. These tests were done previous to summer 2005, and the results were used in subsequent testing.

In addition to these global PMT tests, specialty tests were done during my summer REU at Fermilab on seven PMTs. The purpose of these tests is the following. In order for the Monte Carlo simulation to properly model the behavior of the PMTs, it is necessary to correctly include their efficiency as a function of incident photon angle. The dominant effect comes simply from the solid angle subtended by a PMT as a function of angle, and this is handled by coding an approximate PMT shape into the simulation. Any remaining efficiency function must be measured and entered into the code. The measurement, however, will itself contain the solid angle effects; these must be factored out of the measured angular efficiency to avoid double-counting. A thorough understanding of the angle-dependent response, time and charge resolution, and individual variations of the photomultiplier tubes will help accurately identify neutrino events within the MiniBooNE detector.

The main objective of the angular tests was to find how the response of the PMTs depended on the angle of incident light. There were three additional tests. One tested a few tubes at various voltages. Another rotated the tubes about two orthogonal axes arbitrarily labelled “yaw” and “pitch” to test the assumption that the tubes are rotationally symmetric. The last tested tubes in air, without the oil present in the other tests. The angular dependence data from R1408 and R5912 tubes were kept separate until the final analyses.

## 1 Apparatus

The apparatus used for these tests is designed to replicate as closely as possible the characteristics of the MiniBooNE detector, on a much smaller and more manageable scale. The central part of the apparatus is a 40 gallon, stainless steel tank, painted on the inside with the paint used in the detector tank: a primer and black top coat. The primer is Hydralon P water-based epoxy primer (Sherwin Williams E72AC500/V66VC503 Hydralon P water-based epoxy primer), and the black topcoat is a flat black moisture cure aliphatic polyurethane chemical agent resistive coating (F93B102 Flat black moisture cure polyurethane). The tank can be filled with MiniBooNE oil when tests require it. It houses a single PMT, which can be rotated along



Figure 1: A typical phototube used in the MiniBooNE detector: an 8 inch R1408 mounted on its wire frame. The base is coated with Masterbond before the PMT is installed into the detector.

the polar or azimuthal angle of the tube, using two precision rotary tables, one for pitch and one for yaw with respect to the table. The tubes were fixed to these tables with an arbitrary rotation, so “pitch” and “yaw” refer only to the mechanical apparatus and not any characteristic of the tubes. These tables have externally-coupled mechanical controls which allow the phototube position angle to be changed without opening the tank and exposing the tube to light. A 10.25 inch diameter window at the front of the tank allows the tests to simulate the light in MiniBooNE events by propagating the light several meters before it strikes the phototube. Because of this window, the entire testing room must be kept dark throughout each test.

The light source is a PicoQuant PLS 450, a sub-nanosecond pulsed LED. Its center wavelength is 460 nm, with 50  $\mu\text{W}$  average power at 40 MHz, approximately 30 nm spectral width, and typically 800 ps pulse width. It was used in 10 second sample periods at about  $10^6$  Hz. The light was filtered to produce a low-intensity beam ( $<1$  photoelectron per pulse). The light was directed through an optical cable to face the tank from a distance of approximately 3 meters. The light from this source makes a cone with half-angle about  $23^\circ$ , with greatest intensity along the centerline. The 3 m distance is great enough that one can assume that the entire face of the tube is uniformly illuminated with light in parallel rays.

The signals from the tube in the testing tank can be read out via an oscilloscope/GPIB card, or via the MiniBooNE data acquisition system. For the angular tests, a specialized data acquisition system was used (Fig. 2). The signal from the tube in the tank is amplified by a factor of 100, sent to a discriminator with 30 mV threshold, and finally put into coincidence with the delayed sync out signal from the LED pulser. The number of coincidences and the number of input light pulses each go to a scaler; they are then recorded and used to calculate the relative efficiency.

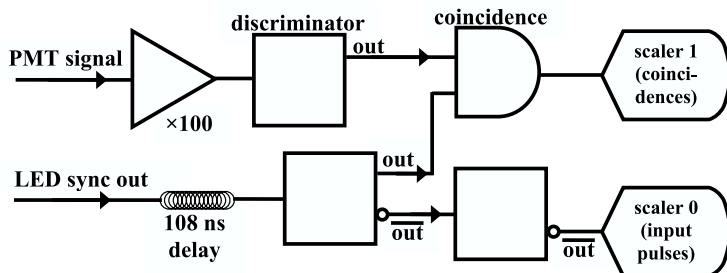


Figure 2: Testing tank data acquisition system block diagram. [5]

The tank is magnetically shielded with a  $\mu$ -metal box. This was done because ambient magnetic fields (e.g., the Earth’s) can influence the relative

efficiency of the tubes, and thus rotation within these fields may change the shape of the relative efficiency results. To see if ambient magnetic fields could have a significant effect, the tank was rotated (while holding the configuration of the tube and internal light source constant). The resulting effect was smaller than (but on the same order as) the angular dependence. When the tank was shielded and the same tests were performed, this dependence on orientation within ambient fields was not seen.

## 2 Procedures

The apparatus detailed above was used to study relative efficiency ( $E_{rel}$ ) as a function of angle. Using rapid, short-duration pulses of the LED, the  $E_{rel}$  of the tube was measured at a given position by taking the ratio of the number of responses which coincided with LED pulses to the total number of pulses, with about  $10^7$  pulses per datum.

$$\left( \frac{\text{coincidences out}}{\text{pulsers pulses in}} \right) = \text{relative efficiency } (E_{rel})$$

$E_{rel}$  values were measured at  $5^\circ$  increments through the entire  $360^\circ$  of response, with two repetitions at each point and two rotations of the tube (from  $\theta = -180^\circ$  to  $\theta = +180^\circ$  and back again) for a total of four measurements at each tube position. Data were recorded directly into a spreadsheet, providing an ongoing real-time check.

This rotational test was performed on four R1408 and three R5912 tubes. Most of these tubes had been previously tested with the global testing, so the expected dark rate was known, and known to be comparable to that for the other tubes. The global testing results also specified tube operating voltages. It was necessary to dark adapt each tube for at least 12 hours to obtain a dark rate comparable to that of the tubes in the detector, which have not been exposed to bright light for over three years.

The phototubes are essentially rotationally symmetric about their central vertical axis, with variation only in the dynode structure below the main dome. The R1408 tubes have “venetian blind” style dynodes; the R5912 tubes have “box and line” style dynodes. No significant differences were observed when the dynodes at the starting position were oriented horizontally, vertically, or at  $45^\circ$ . Additionally, a test was performed on one tube varying the yaw angle (similar to the pitch measurements performed on all tubes); again no significant differences were observed. The equivalence of pitch and yaw implies that the roll orientation of the tube does not affect the results. This simplified the measurements greatly.

Another test was performed by varying the operating voltages by 50 V above and below the nominal voltages found by previous MiniBooNE tests. The gain variation with voltage, which determines the max  $E_{rel}$ , was already known, so this test checked for variation in the shape of the  $E_{rel}$  curve more than the expected variations in amplitude. None of significance was observed.

### 3 Results

Plots of relative efficiency as a function of angle were made for each set of measurements; these are roughly bell-shaped, as one would expect from the shape of the tubes. Typical results from an R1408 and an R5912 (with the fits as described below) are included in Figures 3 and 4. These plots are similar from tube to tube (see Figure 5). The parameters for the fits, as well as the average which will be used in the MiniBooNE Monte Carlo simulation, are included in Table 1. The results obtained were compared to expectations from the shape of the PMTs and results obtained by the SNO [6] experiment.

The initial data were analyzed in the following way. Because the PMT rotator mount inside the tank does not precisely specify the initial angle, max  $E_{rel}$  is found for each curve; the angle corresponding to max  $E_{rel}$  is assumed to correspond to  $\theta = 0$ . Each plot's horizontal axis is shifted accordingly before the plots are compared. Each y-axis is scaled to max  $E_{rel} = 1$ . An initial quadratic fit is performed on the central points of each plot to determine the horizontal shift. A 6-degree polynomial fit is then performed on each plot in the region  $\theta = -150^\circ$  to  $\theta = 150^\circ$ . Outside of this region, statistics were significantly lower, making the data less comparable from tube to tube. The fit polynomial is forced to be symmetric by employing only even powers of the incident angle. The polynomial coefficients are varied to minimize the  $\chi^2$ . Finally, before comparing the functions, each fit is normalized by dividing by its constant term (which equals max  $E_{rel}$ ), forcing max  $E_{rel} = 1$ . The results of the fits are shown in Table 1 and superimposed on Figures 5 and 9.

The errors on these data are dominated by tube-to-tube variation. The tests on each tube individually had very high statistics, typically around  $2 \times 10^7$  light pulses at each measured angle, and about 600 000 responses at central angles or 4 000 at extreme angles (where the tube was facing backwards). Thus, to describe the error, it is more important to look at the relatively large differences between data sets from different tubes. This was done by examining the parameters of the fits. The average of the seven fitted values of each parameter and their standard deviation from that average are given in Table 1. Figure 5 compares each PMT to the average fit, and

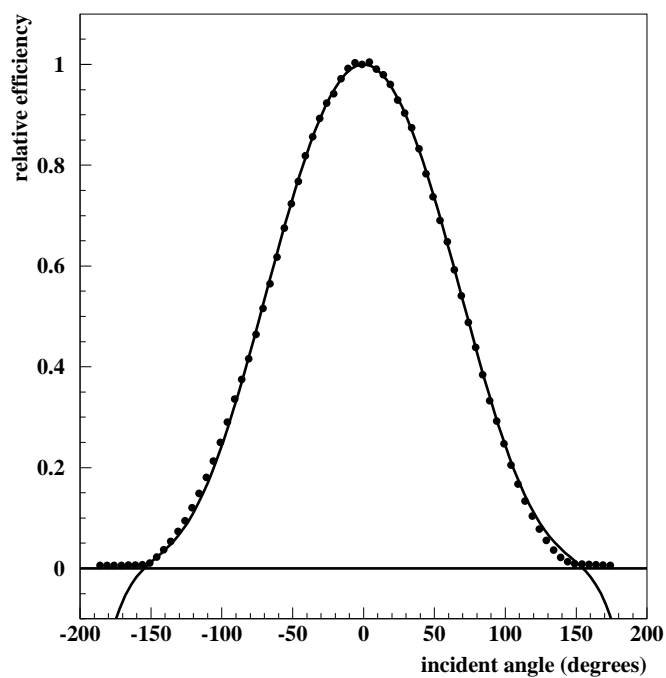


Figure 3: A typical data set from an R1408 tube (19s3) with its symmetric polynomial fit. This fit uses the horizontal shift and maximum relative efficiency found from the initial quadratic fit.

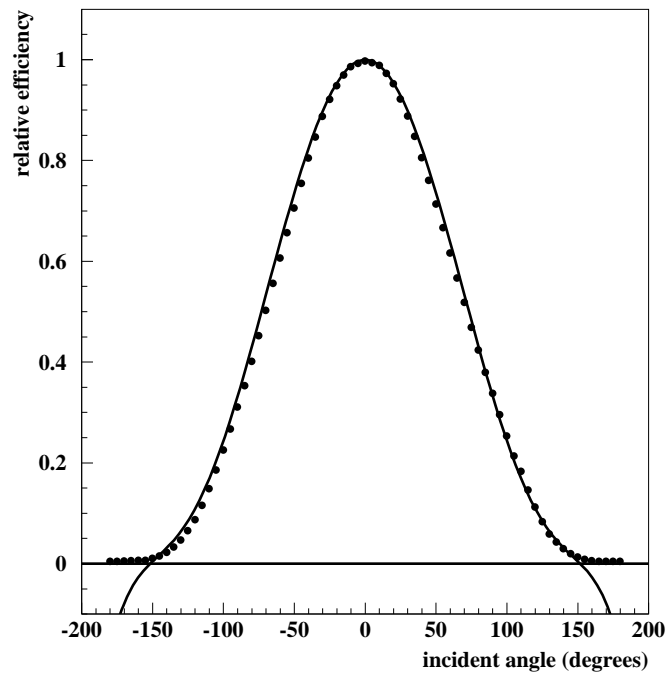


Figure 4: A typical data set from an R5912 tube (SA2761) with its symmetric polynomial fit, analogous to Figure 3.

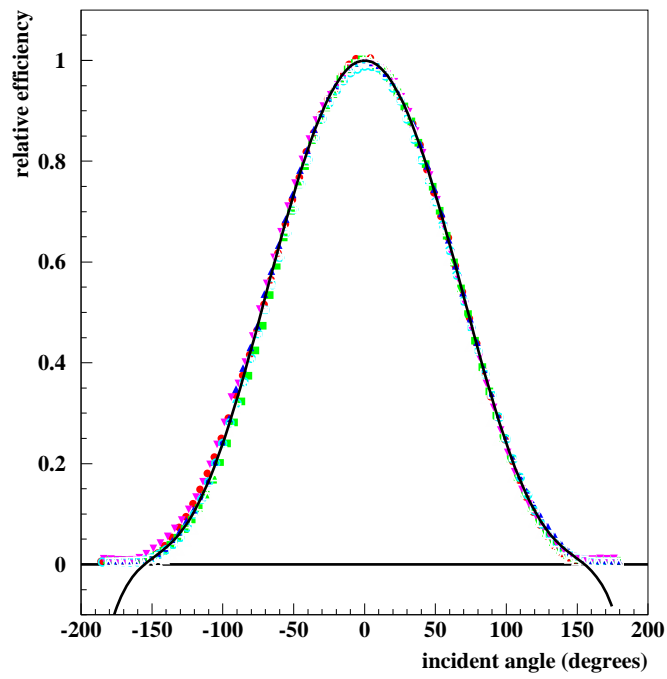


Figure 5: Composite relative efficiency data. The data in each series were fitted to a polynomial, and normalized to  $\max E_{rel} = 1$  at  $\theta = 0^\circ$ . The average fit is shown.

Table 1: Normalized parameters from all all tubes tested. The error is the standard deviation from the average of the seven tubes tested. These parameters are to be used in the following function for the Monte Carlo simulation, where  $\theta$  is the angle of the incident light from the tube axis measured in degrees.

$$E_{rel} = 1 + a_2\theta^2 + a_4\theta^4 + a_6\theta^6.$$

tube number	$a_2$	$a_4$	$a_6$
15s3	$-1.182 \times 10^{-4}$	$5.018 \times 10^{-9}$	$-7.624 \times 10^{-14}$
19s3	$-1.234 \times 10^{-4}$	$5.436 \times 10^{-9}$	$-8.468 \times 10^{-14}$
20s1	$-1.162 \times 10^{-4}$	$4.818 \times 10^{-9}$	$-7.136 \times 10^{-14}$
20n16	$-1.156 \times 10^{-4}$	$4.725 \times 10^{-9}$	$-6.728 \times 10^{-14}$
SA2753	$-1.101 \times 10^{-4}$	$4.191 \times 10^{-9}$	$-5.539 \times 10^{-14}$
SA2761	$-1.177 \times 10^{-4}$	$4.964 \times 10^{-9}$	$-7.552 \times 10^{-14}$
SA2272	$-1.264 \times 10^{-4}$	$5.563 \times 10^{-9}$	$-8.549 \times 10^{-14}$
average	$-1.182 \times 10^{-4}$	$4.959 \times 10^{-9}$	$-7.371 \times 10^{-14}$
error	$5.337 \times 10^{-6}$	$4.583 \times 10^{-10}$	$1.042 \times 10^{-14}$
% error	4.5	9.2	14.1

deviations from the average fit are shown in Fig. 6.

The even-polynomial fits are sufficiently accurate and consistent for the R1408 tubes. For the R5912 tubes, the fits are less accurate on one side (see Figure 4). To describe this difference, several other fits of the R5912 tube data were attempted. The main attempted non-symmetric fits used a different 5-degree polynomial for angles above or below zero, requiring only that they meet at  $\theta = 0$ . The same horizontal shift and max  $E_{rel}$  were used for this fit as for the initial, even polynomial fit. However, it was found that the variation between individual tubes was larger than the average difference between R5912 tubes and R1408 tubes, so the even polynomial fit was used for all tubes.

## 4 Comparison to predictions and to SNO data

MiniBooNE's relative efficiency angular data were compared to several geometrical models, and to data from previous tests from the Sudbury Neutrino Observatory (SNO) experiment [6]. The three geometrical models assumed the photocathode was a flat disk, a hemisphere, and the shape from the

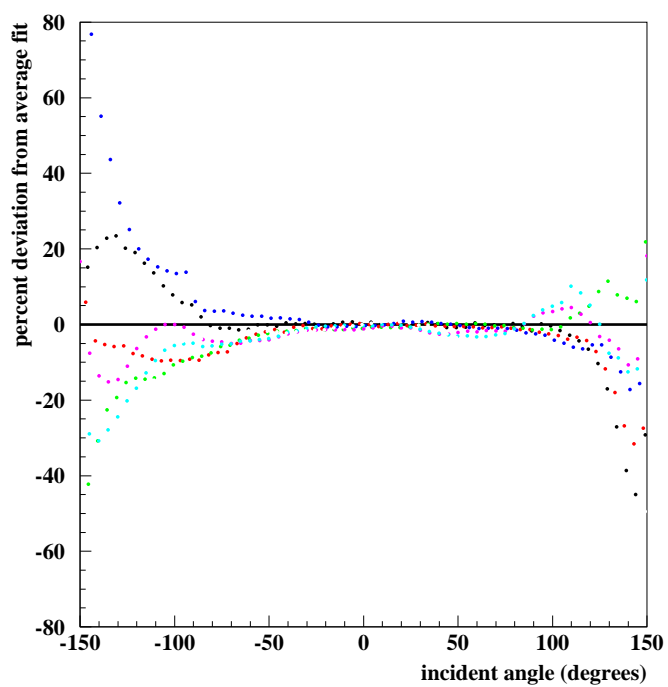


Figure 6: Comparison of the data for each tube to the average fit. This plot shows, for each tube, the percent difference between the data and the average fit (i.e.,  $100 \times (E_{rel} - f(\theta))/f(\theta)$ ).

Hamamatsu technical specifications. The data from SNO were taken from tests on two R1408 PMTs in air and water, for a total of four tests. The PMTs in their detector are all Hamamatsu R1408 PMTs (the same as the MiniBooNE R1408 tubes), making comparisons with them particularly useful. These seven results are shown together in Figure 7. Note that all of the SNO results lie between the hemisphere and the ovoid shape predictions on the top and the flat disk prediction on the bottom. SNO used water instead of oil because the SNO detector contains water.

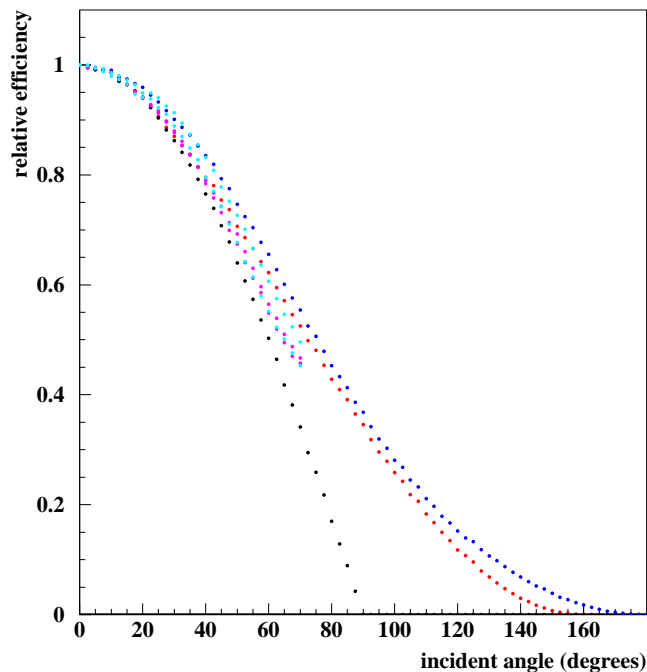


Figure 7: Relative efficiency predicted by assuming that the PMT is a flat disk (black), a hemisphere (red), or ovoid shaped as in the Hamamatsu technical drawing (figure ??) (blue), and the results found by SNO from testing two PMTs each in air (purple) and water (cyan).

While developing the testing procedure, one tube was tested without filling the testing tank with oil. The results from this test, normalized to  $\max E_{rel} = 1$ , were very similar to the air tests done by SNO. This comparison is shown in Figure 9.

Comparisons among the angular response measurements, SNO data, and geometrical models reveal overall similarities. The present data are also observed to be closer to the geometrical model from the Hamamatsu ovoid

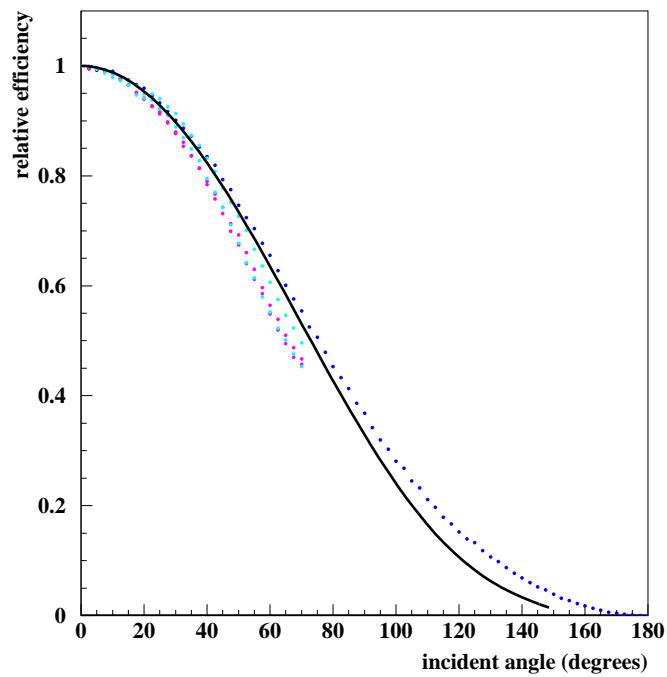


Figure 8: Comparison of the average MiniBooNE  $E_{rel}$  function (black curve) with the SNO results from testing two PMTs each in air (purple) and water (cyan) and the geometrical  $E_{rel}$  function based on the Hamamatsu drawing (blue points).

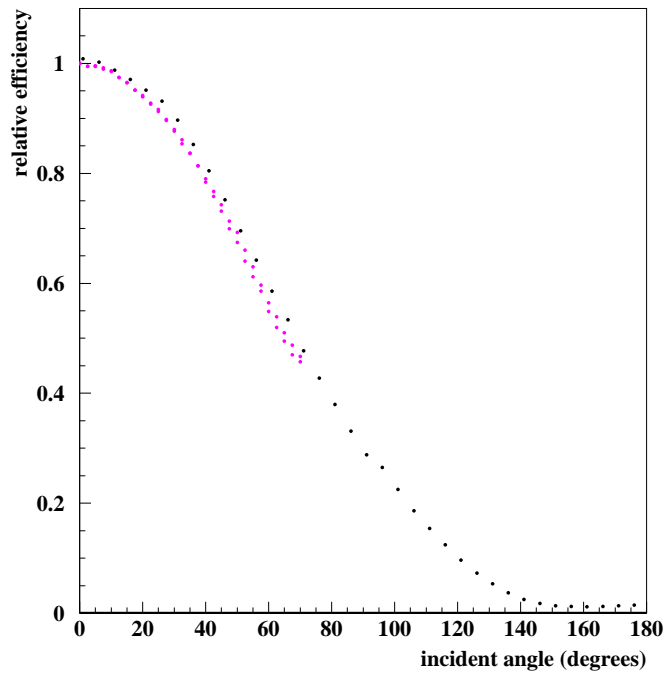


Figure 9: Comparison of MiniBooNE data from the tube tested in air (black) to SNO test data taken in air (purple).

shape description than to the results obtained in either air or water by SNO. This may be the case because these data were taken in oil, where the index of refraction is much closer to that of glass than either air or water, resulting in less reflection at the oil-glass interface.

## 5 Conclusion

This paper has reported on angular tests of the R1408 and R5912 photomultiplier tubes used in the MiniBooNE experiment. The angular response of the tubes determined a sixth order polynomial function describing the angular response. This resultant fit made sense when compared to similar data and geometric predictions.

## References

- [1] Proposal for the MiniBooNE experiment: <http://www-boone.fnal.gov/publicpages/proposal.ps>.
- [2] C. Athanassopoulos *et al.* [LSND Collaboration], Phys. Rev. Lett. **77**, 3082 (1996) [arXiv:nucl-ex/9605003].
- [3] Hamamatsu Catalog, “Large Photocathode Area PMTs”, Catalog No.TPMH1286E02.  
<http://usa.hamamatsu.com/>  
<http://www.hpj.co.jp/Eng/main.htm> .
- [4] B. T. Fleming, L. Bugel, E. Hawker, V. Sandberg, S. Koutsoliotas, S. McKenney and D. Smith, IEEE Trans. Nucl. Sci. **49**, 984 (2002).
- [5] J. May, M. Wysocki, L. Bugel, B.T. Fleming, P. Nienaber, and D. Smith, Nuclear Science Symposium Conference Record, IEEE, **1**, 10-16 Nov. 2002, pp. 446-449, vol. 1.
- [6] M.T. Lyon, PhD thesis, University of Oxford 59 (2002).